

This is the peer reviewed version of the following article:

Allele specific CRISPR/Cas9 editing of dominant Epidermolysis Bullosa Simplex in human epidermal stem cells / Cattaneo, C; Enzo, E; De Rosa, L; Sercia, L; Consiglio, F; Forcato, M; Bicciato, S; Paiardini, A; Basso, G; Tagliafico, E; Paganelli, A; Fiorentini, C; Magnoni, C; Latella, M C; De Luca, M. - In: MOLECULAR THERAPY. - ISSN 1525-0016. - 32:2(2024), pp. 372-383. [10.1016/j.ymthe.2023.11.027]

*Terms of use:*

The terms and conditions for the reuse of this version of the manuscript are specified in the publishing policy. For all terms of use and more information see the publisher's website.

02/05/2026 23:18

(Article begins on next page)

# Journal Pre-proof

Allele specific CRISPR/Cas9 editing of dominant Epidermolysis Bullosa Simplex in human epidermal stem cells.

C. Cattaneo, E. Enzo, L. De Rosa, L. Sercia, F. Consiglio, M. Forcato, S. Bicciato, A. Paiardini, G. Basso, E. Tagliafico, A. Paganelli, C. Fiorentini, C. Magnoni, M.C. Latella, M. De Luca

PII: S1525-0016(23)00660-3

DOI: <https://doi.org/10.1016/j.ymthe.2023.11.027>

Reference: YMTHE 6251

To appear in: *Molecular Therapy*

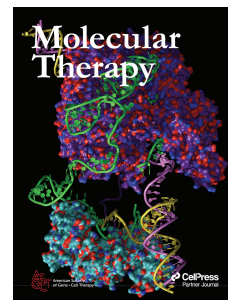
Received Date: 22 May 2023

Accepted Date: 30 November 2023

Please cite this article as: Cattaneo C, Enzo E, De Rosa L, Sercia L, Consiglio F, Forcato M, Bicciato S, Paiardini A, Basso G, Tagliafico E, Paganelli A, Fiorentini C, Magnoni C, Latella MC, De Luca M, Allele specific CRISPR/Cas9 editing of dominant Epidermolysis Bullosa Simplex in human epidermal stem cells., *Molecular Therapy* (2024), doi: <https://doi.org/10.1016/j.ymthe.2023.11.027>.

This is a PDF file of an article that has undergone enhancements after acceptance, such as the addition of a cover page and metadata, and formatting for readability, but it is not yet the definitive version of record. This version will undergo additional copyediting, typesetting and review before it is published in its final form, but we are providing this version to give early visibility of the article. Please note that, during the production process, errors may be discovered which could affect the content, and all legal disclaimers that apply to the journal pertain.

© 2023 The Author(s).





1 **Allele specific CRISPR/Cas9 editing of dominant Epidermolysis Bullosa Simplex in human**  
2 **epidermal stem cells.**

3 Cattaneo C.<sup>1</sup>, Enzo E.<sup>1</sup>, De Rosa L.<sup>1</sup>, Sercia L.<sup>1</sup>, Consiglio F.<sup>2</sup>, Forcato M.<sup>3</sup>, Bicciato S.<sup>3</sup>,  
4 Paiardini A.<sup>4</sup>, Basso G.<sup>5</sup>, Tagliafico E.<sup>6</sup>, Paganelli A.<sup>7</sup>, Fiorentini C.<sup>7</sup>, Magnoni C.<sup>7</sup>, Latella M.C.\*<sup>2</sup>,  
5 De Luca M.\*<sup>1</sup>.

6 \* These authors contributed equally to this work.

7 **Affiliations**

- 8 • <sup>1</sup> Centre for Regenerative Medicine "Stefano Ferrari", Department of Life Sciences,  
9 University of Modena and Reggio Emilia, 41125, Modena, Italy.
- 10 • <sup>2</sup> Holostem Terapie Avanzate, s.r.l., 41125, Modena, Italy.
- 11 • <sup>3</sup>Department of Life Sciences, University of Modena and Reggio Emilia, 41125, Modena,  
12 Italy.
- 13 • <sup>4</sup>Department of Biochemical Sciences 'A. Rossi Fanelli', Sapienza Università di Roma,  
14 Rome, 00185, Italy.
- 15 • <sup>5</sup> Genomic Units, IRCCS Humanitas Research Hospital, 20089, Rozzano, Milan, Italy
- 16 • <sup>6</sup>Department of Laboratory Medicine and Pathology, Diagnostic hematology and Clinical,  
17 Genomics Unit, Modena University Hospital, 41124, Modena, Italy.
- 18 • <sup>7</sup> Regenerative and Oncological Dermatological Surgery Unit, Modena University Hospital,  
19 41124 Modena, Italy.

20 Correspondence should be addressed to M.D.L.: [michele.deluca@unimore.it](mailto:michele.deluca@unimore.it); tel. +39 059  
21 2058057; Fax. +39 059 2058115

22

23

## 24 **Abstract**

25 Epidermolysis Bullosa Simplex (EBS) is a rare skin disease inherited mostly in an autosomal  
26 dominant manner. Patients display a skin fragility that leads to blisters and erosions caused by minor  
27 mechanical trauma. EBS phenotypic and genotypic variants are caused by genetic defects in  
28 intracellular proteins whose function is to provide the attachment of basal keratinocytes to the  
29 basement membrane zone and most of EBS cases display mutations in keratin 5 (*KRT5*) and keratin  
30 14 (*KRT14*) genes. Besides palliative treatments, there is still no long-lasting effective cure to correct  
31 the mutant gene and abolish dominant negative effect of the pathogenic protein over its wild-type  
32 counterpart. Here, we propose a molecular strategy for EBS01 patient's keratinocytes carrying a  
33 monoallelic c.475/495del21 mutation in *KRT14* exon1. Through the CRISPR/Cas9 system we  
34 performed a specific cleavage only on the mutant allele and restore a normal cellular phenotype and  
35 a correct intermediate filament network, without affecting the epidermal stem cell, referred to as  
36 holoclones, which play a crucial role in epidermal regeneration.

## 37 **Introduction**

38 Inherited EB is a heterogeneous group of rare, autosomal genetic disorders caused by molecular  
39 defects within genes encoding structural proteins forming the epidermal–dermal junction. EB is  
40 characterized by recurrent blistering and erosions of the skin (and other stratified epithelia) that arise,  
41 spontaneously or upon minimal mechanical stress, within the epidermis in EB simplex (EBS), the  
42 lamina lucida in Junctional EB (JEB) and beneath the lamina densa in Dystrophic EB (DEB). EBS is  
43 the most common EB form, with a prevalence of 1/30000 - 1/50000.<sup>1,2</sup> Its clinical manifestations are  
44 usually less severe than those of JEB and DEB, which can be devastating and even early lethal.  
45 However, some EBS forms are marked by a severe phenotype and several clinical variants have been  
46 identified based on the mutated gene, site of blister formation, anatomical distribution and mode of  
47 inheritance.<sup>3-5</sup>

48 JEB and DEB are mostly recessively inherited, whilst the vast majority of EBS are inherited in a  
49 dominant manner. In fact, approximately 75% patients suffering from EBS harbours dominant  
50 mutations in *KRT5* and *KRT14*, the genes encoding keratin 5 (K5) and keratin 14 (K14), respectively.  
51 K5/K14 pairs form the basal keratinocyte intermediate filaments, which are part of the  
52 hemidesmosomal protein complex tethering the epidermal basal layer to the basement membrane and  
53 the underlying dermis. Mutant keratins exert a dominant negative effect on the functional keratins  
54 encoded by the normal allele, hence perturbing the basal keratinocyte intermediate filament network  
55 and leading to intraepidermal blister formation. Thus, whilst JEB and DEB can be tackled by the  
56 addition of a corrected copy of the mutated gene in the genome of epidermal stem cells<sup>6-14</sup>, a  
57 potentially successful combined ex vivo cell and gene therapy of EBS strictly requires editing of the  
58 mutated allele.

59 Here, we outlined an allele specific CRISPR/Cas9 based gene editing approach that is able to disrupt  
60 specifically the *KRT14* mutant gene and fully restore functional intermediate filaments in epidermal  
61 stem cells, cultivated from an EBS patient carrying a *de novo* monoallelic c.475/495del21 dominant  
62 mutation in exon 1 of *KRT14*.

63 This approach takes advantage of a tailored CRISPR/Cas9 system to induce double strand breaks  
64 (DSBs) specifically on the mutant allele, leading to non-homologous end joining (NHEJ) repairing  
65 process. These rearrangements are likely to generate frameshift mutations resulting in both  
66 pathogenic allele expression abolishment and phenotypic and mechanical stress resilience restoration.  
67 Besides the remarkable efficacy of this approach, we also demonstrate the correction of the epithelial  
68 stem cells compartment, which is mandatory for the long-term skin regeneration. This highly effective  
69 and safe gene editing strategy would therefore enable a translation to clinical application for the  
70 treatment of other dominant form of EB.

71

## 72 **Results**

### 73 **Novel monoallelic *KRT14* deletion causing a dominant form of Epidermolysis Bullosa Simplex**

74 An 8-year-old EBS patient (referred to as EBS01) suffered from a *de novo* heterozygous dominant  
75 mutation (c.475/495del21) within exon 1 of *KRT14*. The patient developed bullous skin lesions few  
76 months after birth and currently presents blisters in the palmoplantar region causing postural and  
77 ambulation problems. No other cases of EB were known among his relatives. Besides the palliative  
78 care and a regular multidisciplinary follow-up, no resolutive treatment is available for this patient  
79 (Fig. 1A).

80 The EBS01 variant results in the deletion of seven in-frame amino acids, leading to a shorter K14  
81 protein. The AlphaFold2<sup>15</sup> suite for protein structure prediction and modeling was used to predict the  
82 3D-structure of the shorter K14 (Fig. 1B). The c.475/495del21 variant affects the protein structure  
83 resulting in the absence of an extended loop, Linker L1, encompassing residues 159–165 (Fig. 1B).<sup>16</sup>  
84 The L1 structural motif of K14, whose function is still poorly characterized, is predicted to assume a  
85 highly flexible, non-helical  $\beta$ -turn, with the pivotal function of connecting coil 1A with 1B (Fig.  
86 1C).<sup>17</sup> The importance of the L1 motif is also reflected by its high evolutionary conservation in  
87 keratins.<sup>18</sup> Indeed, mutations affecting the linker regions of intermediate filaments have been  
88 previously observed and related to severe cases of inherited skin blistering diseases, highlighting the  
89 unexpected sensitivity of these regions to structural alterations.<sup>17</sup>

90

### 91 **Efficient and precise *KRT14* allele-specific editing in EBS primary keratinocytes**

92 The EBS01 genetic variation enables the mutant K14 to exert a dominant negative effect over its  
93 wild-type counterpart expressed by the other allele. Thus, a tailored CRISPR/Cas9 system was  
94 employed to target the monoallelic *de novo* mutation (c.475/495del21) within exon 1 of *KRT14* to  
95 induce a deleterious double strand break on the mutant allele and promote NHEJ, inducing specific

96 disruption of the mutant *KRT14* open reading frame. We designed a sgRNA tailored to specifically  
97 target only the mutant *KRT14* allele and employed the SpCas9 to specifically recognize the “NGG”  
98 PAM present near the deletion site. For the desired specificity, the 19 nucleotides long guide RNA  
99 was sketched straddling both the terminal sides of the 21 base pair deletion and directly flanking the  
100 “AGG” PAM sequence within its 3’ end (Fig. 2A).

101 To first assess the ability of the designed CRISPR/Cas9 system to specifically abolish the expression  
102 of the *KRT14* mutant allele, preliminary experiments employed a lentiviral vector to deliver the gene  
103 editing machinery to EBS01-derived primary keratinocytes.

104 Strikingly, the gene editing machinery was able to disrupt the expression of the mutant *KRT14* allele  
105 with an efficiency up to 94%, without affecting the wild-type allele (Fig. S1A). We then performed  
106 an *in silico* genome analysis to assess the site specificity of sgRNA\_del21 using Cas-OFFinder,  
107 followed by CCTop and COSMID. We could not detect off-target sites with either none or single  
108 mismatch and DNA bulge size=0. However, introducing 2 random mismatches led to the discovery  
109 of 2 potential off-targets, both located in intergenic sequences. When 3 random mismatches were  
110 introduced, we identified a total of 86 potential off-targets. The majority of these off-target sites were  
111 found in intergenic regions (41) and introns (44), with only one potential off-target located in a coding  
112 region (3’ untranslated region of *ZNF641* gene). We focused on six off-targets out of these candidates,  
113 based on their potential relevance to gene function in the epidermis.

114 TIDE analysis outlined the presence of unwanted cleavage in one of the predicted off-target sites  
115 (Fig. S1B). These preliminary data suggested that the editing strategy designed to tackle the EBS01  
116 mutation is indeed appropriate.

117 Lentiviral-mediated genome integration of the CRISPR/Cas9 components and their constitutive  
118 expression may increase off-target cleavage of similar genomic sequences overtime and trigger  
119 unwanted immunological response due to the Cas9 bacterial origin.<sup>19</sup> In fact, stable genome

120 integration of the lentiviral-mediated gene editing cassette is neither needed, nor desirable for clinical  
121 application, in that transient expression of both endonuclease and guide RNA is sufficient to attain a  
122 stable gene editing.

123 However, human keratinocytes are hard to transfect and genome access turns out to be a major issue.  
124 Thus, different transfection methods were attempted to deliver the gene editing machinery into  
125 EBS01 keratinocytes.

126 Plasmids expressing CRISPR/Cas9 components were initially delivered into cells using commercial  
127 lipofectamine reagents, which turned out to be highly inefficient. To implement the transfection  
128 efficacy and assure an optimal editing efficiency, additional electroporation procedures were  
129 investigated, all of which were highly toxic for normal human keratinocytes (data not shown).

130 To overcome these hurdles, EBS01 primary keratinocytes were directly electroporated with a  
131 ribonucleoprotein complex (RNP) composed of the SpCas9 endonuclease protein and the guide RNA  
132 specific for the mutant allele (sgRNA\_del21) (sequence in Table S1).

133 Following RNP nucleofection, edited EBS01 keratinocytes (eEBS01) underwent further analysis to  
134 characterize genotypically and phenotypically the editing impact, always comparing them with a not  
135 transfected EBS01 sample.

136 Genomic DNA was extracted from sub-confluent eEBS01 and EBS01 cultures and the locus around  
137 the 21 base pair deletion was amplified by PCR and used to perform Sanger sequencing. The amplicon  
138 sequences were analysed using TIDE analysis (sensitivity >1-5%) and validated with next-generation  
139 sequencing (NGS).

140 As shown in Figure 2B, TIDE analysis outlined a strikingly high allele specificity of our tailored gene  
141 editing approach. In eEBS01 cells, the wild-type allele was virtually untouched, whereas the mutant  
142 allele displayed a significant amount of InDels abolishing the open reading frame and expression of

143 pathogenic K14. NGS analysis of three independent RNP nucleofections confirmed the remarkable  
144 allele specificity (Table S2), with a mutant allele specific gene editing greater than 95% (Fig. 2C).

145 Of note, ddPCR (Fig. S2A) and western blot analysis (Fig. S2B) showed that editing of the mutant  
146 allele restored both *KRT14* mRNA and K14 expression in eEBS01 keratinocytes, as compared to  
147 EBS01 cells. Gene editing specificity was confirmed in an agarose gel analysis, in which PCR  
148 products were amplified with oligonucleotides specific for the wild-type (268 bp) and mutant alleles  
149 (266bp). As shown in Figure 2D, the introduction of several mismatches, after editing and error prone  
150 DNA repair, caused the inability of the forward mutant allele specific oligonucleotide  
151 (*KRT14\_seq\_del21* primer, see Table S1) to anneal in the edited region, determining the formation  
152 of a feebler eEBS01 mutant allele amplification product. Finally, NGS data were employed to  
153 calculate the frequency of deletion, insertion and substitution in eEBS01 keratinocytes, outlining  
154 deletion as the most frequent modification type (75%), whereas insertion and substitution were  
155 detected at a lower frequency (19% and 6% respectively) (Fig. 2E). An independent analysis of the  
156 NGS data was performed to gain insights into the prevalence of out-of-frame sequences (80% of the  
157 total sequences). The most frequent specific rearrangements are illustrated in Figure 2F.

158

### 159 **Off-Target analysis supports RNP complex-mediated editing specificity and safety**

160 To properly address safety issues, a comprehensive analysis assessing potential off-target sites was  
161 performed. Genomic DNA purified from sub-confluent EBS01 keratinocytes electroporated with the  
162 RNP complex was used to amplify and sequence off-target genomic regions previously identified  
163 after lentiviral transduction. TIDE analysis of eEBS01 shows no undesirable changes in any of the 6  
164 predicted off-target sites, including *PPFIBP1*, thus recovering the unwanted cut chance determined  
165 by the genomic lentiviral vector-mediated integration and stable expression of the CRISPR/Cas9  
166 components (Fig. S3).

167 Unbiased genome wide GUIDE-seq analysis was carried-out, the DNA library was sequenced using  
168 Illumina Miseq. The subsequent datasets were analysed using GUIDE-seq Bioconductor package  
169 software. The analysis confirmed preservation of the *KRT14* wild-type allele but outlined 9 “putative”  
170 off-target sites with a frequency below 3% but above 1% (Table S3). However, the vast majority of  
171 the implicated gene regions are either intergenic or intronic. The unique coding region involved is  
172 attributed to the *ZNF320* gene, whose expression is anyhow low in basal and superbasal keratinocytes  
173 and with a very low GUIDE-seq predicted editing rate. We NGS validated two off-target sites  
174 identified in intronic regions (*MIPOL* and *BAIAP*) and in the only coding region (*ZNF320*) detected  
175 with GUIDE-seq, for which we obtained appropriate quality PCR products. NGS showed editing  
176 efficiencies of 4.1%, 5.3%, and 6.9% for these respective targets (Table S3; NGS raw data published  
177 on GSE246345).

178 Overall, this data indicates the presence of a small number of potential off-target sites, which have a  
179 minimal effect on gene function, underscoring the safety of this non-viral CRISPR/Cas9 approach.

180

### 181 **Editing of *KRT14* mutant allele restores functional intermediate filament network in EBS01** 182 **keratinocytes**

183 Given the role of K5/K14 pairs in the assembly of keratinocyte intermediate filaments, we  
184 investigated whether the unmodified wild-type *KRT14* allele would suffice in restoring normal  
185 structural and functional phenotype in edited keratinocytes.

186 Healthy donor (NHEK), eEBS01 and EBS01 keratinocytes were seeded onto glass coverslips.  
187 Immunostained colonies clearly showed that corrected eEBS01 keratinocytes contained a properly  
188 functioning intermediate filament network, virtually indistinguishable from that of healthy NHEK.  
189 Keratin filaments were well organized and capable of branching throughout the plasma membrane.  
190 In contrast, EBS01 cells displayed a pathologic, roughly fragmented keratin pattern (Fig. 3A). We  
191 have analysed the intermediate filament assembly in 636 NHEK, 722 EBS01 and 1090 eEBS01 cells.

192 Such analysis is summarized in Fig. S4 (panel D). The magnified areas shown in Fig. S4 (A-C) are  
193 strictly representative of the several images that we have analysed in several independent  
194 experiments. This data confirmed the efficacy of this gene editing approach in restoring EBS altered  
195 cellular phenotype. Of note, the ablation of the mutant *KRT14* allele results in *KRT14*  
196 haploinsufficiency, which is comparable to the condition characterizing healthy carriers of recessive  
197 EBS mutations, who are completely asymptomatic.<sup>20-22</sup>

198 Additional functional assays evaluated the regain of mechanical strength in eEBS01 keratinocytes,  
199 which is mandatory for a more comprehensive validation of an appropriate functional correction.<sup>23</sup>

200 Heat shock assay is one of the easiest and most reproducible tests demonstrating the instability and  
201 thermal sensitivity of mutant keratins in EBS cells. The transient increase in thermal energy of the  
202 system results in evident depolymerization and impairment in affected keratinocytes' filament  
203 network remodelling, which may render cells vulnerable to cytolysis *in vivo* and support the increased  
204 EBS blisters formation in warm environments.<sup>24</sup>

205 To this end, EBS01, eEBS01 and NHEK keratinocyte colonies were submitted to thermal shock. At  
206 time zero and fifteen minutes after heat shock, EBS01 keratinocyte's intermediate filaments showed  
207 an increased disruption of keratin filaments, particularly nearby the nuclear region, which was  
208 partially recovered approximately 60 minutes after thermal shock, with aggregates limited to a small  
209 portion of the cytoplasm.<sup>25,26</sup> Such cytoplasmic aggregates persistence was not observed in NHEK  
210 or eEBS01 (Figure 3B).

211 Since intermediate filaments also play a role in controlling cell mechanical stress, cultured epidermal  
212 sheets prepared from NHEK, EBS01 and eEBS01 were detached from the vessel by incubation with  
213 Dispase II protease (Fig. 3C). EBS01 cultured sheets disintegrated into small pieces when subjected  
214 to high inversion force, whereas eEBS01 sheet showed a structural compactness comparable to that  
215 of the healthy donor (NHEK) (Fig. 3D). The greater eEBS01 mechanical strength was also  
216 quantitatively evaluated counting sheet-derived fragments and confirmed that specific deletion of the

217 mutated *KRT14* allele confers to eEBS01 cells the capability to reassemble proper and resistant  
218 cohesive structures (Fig. 3E).

219  
220 **Edited eEBS01 cells revert the disease phenotype in skin equivalents**

221 We have generated human skin equivalents containing dermal and epidermal compartments  
222 resembling morphological characteristics of human skin. This was achieved by cultivating  
223 keratinocytes on a decellularized human dermal matrix.

224 Figure 4A shows haematoxylin/eosin staining of sections of decellularized dermal matrixes without  
225 cells (Dermis) and those overlaid by a fully stratified epidermis (NHEK). Figure 4B (left panels)  
226 illustrates the decellularized dermal matrix seeded with EBS01 cells. The regenerated epidermis  
227 shows the presence of blisters within the epidermal basal layer (at arrows). In contrast, no blisters  
228 were observed in the epidermis generated by gene-edited eEBS01 keratinocytes (Figure 4B, right  
229 panels).

230 In summary, these results show that the allelic-specific gene editing of mutant *KRT14* restores proper  
231 expression of K14 and functional intermediate filaments in primary clonogenic EBS keratinocytes.

232  
233 **CRISPR/Cas9-mediated gene editing via RNP complex electroporation preserves epidermal**  
234 **stem cells**

235 Epidermal regeneration and repair processes rely on long-lived stem cells producing short-lived  
236 transient amplifying (TA) progenitors that eventually give rise to terminally differentiated  
237 keratinocytes. Keratinocyte stem cells and TA progenitors are located in the basal layer of all stratified  
238 epithelia and generate different clonal types, referred to as Holoclones and Meroclones/Paraclones  
239 respectively.<sup>27-31</sup> In view of future clinical applications, the essential feature of any cultured epithelial  
240 graft is an adequate number of Holoclones-forming cells, which are mandatory for a stable long-term  
241 regeneration of all squamous epithelia.<sup>10,29,32-34</sup> Clonal analysis of EBS01 clonogenic keratinocytes

242 confirmed the presence of each clonal type in the culture (Holoclones, Meroclones and Paraclones),  
243 excluding an impact of this *de novo* mutation on the EBS01 derived keratinocyte stem cell  
244 compartment.

245 To first investigate a potential impact of gene editing on the distribution of the different keratinocyte  
246 clonal types, we took advantage of single keratinocyte RNA sequencing analysis. To this end, we  
247 performed transcriptomic profile analysis of EBS01 and eEBS01 keratinocytes following the same  
248 pipeline recently published<sup>28</sup>, obtaining 5,350 and 7,200 cells, respectively. As reported, both samples  
249 contained the previously identified 5 keratinocytes clusters (Fig. 5A-C), three of which expressed  
250 clonogenic markers (Holoclones, Meroclones and Paraclones clusters), the other two expressing  
251 differentiation markers (Terminally differentiated 1 and 2 clusters) (Fig. S5A-B). In particular, the  
252 Holoclone (stem cell) cluster displayed a “holoclone signature” able to distinguish it from the other  
253 clusters (Fig. S5A-B).

254 To further investigated whether Holoclones were preserved and properly corrected after the gene  
255 editing procedure, two clonal analyses of EBS01 and eEBS01 keratinocytes were performed, as  
256 described in Material and Methods. The classification of the clonal type confirmed the comparable  
257 percentage of Holoclones, Meroclones and Paraclones in both samples (Fig. 5D-E). Genomic DNA,  
258 analysed by PCR amplification using primers specific to amplified wild-type and mutant alleles (see  
259 Table S1) confirmed that holoclone-forming cells have been edited (Fig. 5F).

260 As shown in Supplemental Fig. S6, both clonogenicity (A) and percentage of aborted colonies (B)  
261 (and growth rate) were comparable in long-term cultures generated by EBS01 and eEBS01  
262 keratinocytes, indicating the absence of clonal selection and/or selective advantages of eEBS01  
263 keratinocytes over the EBS01 cells.

264 These data demonstrate that the gene editing procedure was able to preserve and edit the population  
265 of epidermal stem cells crucial to a future *ex vivo* gene therapy aimed at full epidermal restoration.

266

267 **Discussion**

268 Epidermolysis Bullosa simplex (EBS) is a rare mechanobollous disease inherited mainly in an  
269 autosomal dominant fashion and affecting a few thousands of people worldwide. Mutations affecting  
270 *KRT14* account for approximately 30% of the reported cases. Mutant *KRT14* exerts a dominant  
271 negative effect on the normal allele, perturbing the basal keratinocyte intermediate filament network  
272 and leading to intraepidermal blister formation. Hence, a great portion of EBS patients carrying  
273 *KRT14* mutations could potentially benefit from the correction of the genetic defect.<sup>35</sup>

274 Gene replacement strategies, whereby a functional copy of the defective gene is introduced in the  
275 genome of clonogenic keratinocytes, has been successfully exploited in other forms of EB, such as  
276 the *LAMB3*-dependent JEB and RDEB, which are recessively inherited.<sup>6,8,10-13</sup> However, gene  
277 replacement is not appropriate for the treatment of dominantly inherited genetic diseases, which  
278 instead require either the selective disruption of the mutated allele or the precise editing of the specific  
279 mutation.<sup>36,37</sup> An appropriately designed gene editing machinery would allow to discriminate and  
280 inactivate, via error prone NHEJ pathway, only the mutant allele, leaving the wild-type counterpart  
281 functionally intact. Gene editing has been employed to permanently to repair both dominant<sup>38-41</sup> and  
282 recessive<sup>42-44</sup> mutations related to EB using knockout and homologous recombination techniques.  
283 The end-joining pathways, often harnessed for gene knockout, represent the most efficient repair  
284 mechanisms for double-strand breaks.<sup>45</sup> Consequently, gene knockout is the most effective form of  
285 gene editing.

286 This work presents the first evidence of therapeutically relevant allele-specific genetic correction in  
287 primary cultures of EBS-derived epidermal stem cells. CRISPR/Cas9 based allele-specific editing  
288 platform using a guide RNA specific successfully edited a *de novo* c.475/495del21 mutation within  
289 exon 1 of *KRT14* gene in a dominant form of EBS. Our tailored approach was highly effective in  
290 disrupting the mutant *KRT14* allele on EBS01 primary keratinocytes (editing efficiency greater than  
291 95%) with no editing on the wild-type allele. To ensure transient expression of editing machinery

292 suitable for clinical purposes, the sgRNA – Cas9 ribonucleoprotein complex (RNP) has been directly  
293 delivered to EBS01 keratinocytes. Since InDels generation at off-target sites still poses a risk to the  
294 use of engineered nucleases, we also demonstrated a low occurrence of non-specific CRISPR/Cas9  
295 mediated cleavages through unbiased GUIDE-seq analysis.

296 Thus, this approach succeeded in abolishing the mutant *KRT14* allele expression and the pathogenic  
297 keratin almost entirely, and fully restored a functional intermediate filament network. More  
298 importantly, we provide evidence that the long-lived self-renewing stem cells have been targeted and  
299 corrected by the gene editing machinery without any cytotoxicity, thus maintaining the ability to  
300 regenerate a virtually indistinguishable functional epidermis.

301 The selection of a gene editing tool for allele-specific genetic correction depends on factors such as  
302 the specific genetic mutation, the delivery method, the desired level of precision and, perhaps more  
303 importantly, on the cell type, mainly when specific somatic stem cells need to be targeted. In the case  
304 of EBS01 cells, the deletion of 21 base pairs (c.475/495del21) within exon 1 of *KRT14* led us to  
305 design a sgRNA tailored to specifically target the mutant allele. We opted for a gene editing approach  
306 utilizing SpCas9, known for its high cutting efficiency. We have introduced the sgRNA and SpCas9  
307 as a ribonucleoprotein (RNP) complex that overcomes many of the challenges associated with mRNA  
308 delivery, as the translation steps and the folding of the Cas protein. The RNP complex is immediately  
309 active as it is fully developed. Emerging gene editing tools may offer more precise approaches than  
310 traditional methods, but often have an efficiency not sufficient to fully tackle a specific population of  
311 epidermal stem cells, which represent a small percentage of clonogenic keratinocytes. Promising gene  
312 editing tools for allele-specific genetic correction include prime editing<sup>46,47</sup>, base editing<sup>48,49</sup>, and  
313 Cpf1/Cas12-based editing<sup>50-52</sup> which provides versatility by targeting distinct DNA sequences,  
314 widening the scope of targetable genetic mutations. These tools hold great therapeutic promise due  
315 to their precision and reduced off-target effects.

316 In the context of clinical translation and safety of gene editing strategies, a key aspect is the analysis  
317 of off-target effects. As sequencing technologies and data analysis tools continue to advance, there  
318 may be, in the near future, more cost-effective and high-throughput options for off-target analysis  
319 than whole-genome sequencing.

320 Our study provides a clear demonstration of the efficacy and potential safety of an allele-specific  
321 CRISPR based gene editing approach, which we envision to further translate into a long-lasting  
322 decisive clinical treatment for patients suffering from EBS and possibly other related skin-blistering  
323 diseases. Although we did not observe abnormal clonal expansion, clinical translation would require  
324 additional efforts to determine the optimal RNP dosage to achieve maximal on-target efficiency and  
325 minimal off-target impact and thoroughly verify the absence of genotoxicity and genomic  
326 instabilities.

327

## 328 **Materials and Methods**

### 329 **Patient, Clinal data and treatments**

330 EBS patient (EBS01) displayed skin lesions to exclusively the acral regions and no mucosal blisters  
331 nor erosions were ever reported either by him or his parents. Clinical description and genetic  
332 counselling with genetic analysis of the family in Supplemental Materials and Methods.

### 333 **Structural Modeling**

334 The structure predictions were performed in a standalone platform of AlphaFold2 and AlphaFold-  
335 Multimer<sup>15</sup> as implemented in ColabFold, which was set up on a local computer with a Linux  
336 operating system and accelerated with two NVIDIA GeForce RTX 2080 Ti GPU. The “Template  
337 mode” using PDB 3TNU<sup>16</sup> was used for this purpose. The other parameters were kept at their default  
338 values.

**339 Primary human cell culture from Epidermolysis Bullosa Simplex patient**

340 A skin biopsy has been collected from the EBS01 patient, after obtaining the informed consent.  
341 Briefly, skin biopsy was minced and treated with 0,05% trypsin/ 0,01% EDTA for 4 h at 37°C. Every  
342 30 min keratinocytes were collected, plated ( $2,5-3 \times 10^4$  cells/cm<sup>2</sup>) on lethally irradiated 3T3-J2-Y  
343 cells and grown at 37°C, 5% CO<sub>2</sub> in humidified atmosphere in KGM medium: Dulbecco's modified  
344 Eagle's (DMEM) and Ham's F12 media (2:1 mixture) containing fetal bovine serum (FBS) (10%),  
345 penicillin-streptomycin (50 IU/ml), glutamine (4mM), adenine (0,18mM), insulin (5mg/ml), cholera  
346 toxin (0,1nM), hydrocortisone (1,1mM), triiodothyronine (Lithyronine Sodium. 2nM), epidermal  
347 growth factor (EGF, 10ng/ml). When sub-confluent, cell cultures were serially propagated.

**348 3T3-J2 cell line**

349 Mouse 3T3-J2 cells were a gift of Professor Howard Green, Harvard Medical School (Boston MA,  
350 USA).<sup>53</sup> Fibroblasts were cultivated in DMEM supplemented with 10% g-irradiated donor adult  
351 bovine serum, penicillin-streptomycin (50IU/ml) and glutamine (4mM). GmbH, (Idar-Oberstein,  
352 Germany) produce a GMP clinical grade 3T3-J2 cell bank. That have been authorized for clinical use  
353 by national and European regulatory authorities.

**354 Ribonucleoprotein (RNP) complex formation and Nucleofection**

355 The synthetic guide RNA was designed straddling both the terminal sides of the c475/495del21  
356 mutation (5'-GCTGAGGTTCAAGACCATTG-3') and directly flanking an "AGG" PAM. It was  
357 modified to drive the maximum editing efficiency (Invitrogen, #A35514, Table S1) and was mixed  
358 in a 1,1:1 molar ratio with the Cas9 protein (Alt-R S.p. Cas9 Nuclease V3, IDT, #1081058).  $5 \times 10^5$   
359 keratinocytes were resuspended in 100µl primary cell nucleofection solution (P3 Primary Cell 4D-  
360 Nucleofector Kit, Lonza, #LOV4XP3024), mixed with the RNP complex solution and 4µM Cas9  
361 electroporation enhancer (Alt-R Cas9 Electroporation Enhancer, IDT, #1075915). Cells were

362 electroporated using a 4D-Nucleofector (4D-Nucleofector Core Unit, Lonza, #AAF-1001B; 4D-  
363 Nucleofector X Unit, Lonza, #AAF-1001X) using the program DS-138.

#### 364 **Editing analysis by sequence decomposition (TIDE)**

365 eEBS01 and EBS01 keratinocytes genomic DNA was isolated using the QIAamp DNA Mini Kit  
366 (QIAGEN, #51304). A 500 base pair region around eEBS01 and EBS01 genomic target site was  
367 amplified by PCR (primers in Table S1). PCR amplicons were subjected to conventional Sanger  
368 sequencing. The resulting sequence trace files were uploaded on TIDE web tool with the guide RNA  
369 sequence as input.

#### 370 **PCR and allele characterization**

371 Screening of the allele pattern, in eEBS01 and EBS01 keratinocyte, was done by PCR. The  
372 “KRT14\_seq\_del21” forward primer was specific only for the mutant allele in EBS01 keratinocyte,  
373 “KRT14\_seq\_wt” forward primer was specific only for the wild-type allele. Reverse primer was  
374 specific for a sequence common to both alleles (Table S1).

#### 375 **OFF-target analysis**

376 CRISPR/Cas9 online predictors were used to identify the genomic regions which may present the  
377 greatest probability of off-target cuttings. Off-target probability was evaluated on the basis of  
378 mismatches numbers and the genomic loci of the most probable in silico off-target sites were  
379 sequenced and analysed. The resulting sequence trace files were uploaded on TIDE web tool with the  
380 guide RNA sequence as input.

#### 381 **NGS analysis**

382 The region near the target site was amplified by specific PCR primers with sequence adaptor  
383 (Supplementary table 1, KRT14ex1\_NGS and KRT14intr1\_NGS) and 25 µl of purified amplicon was  
384 used to NGS analysis using Illumina sequencing platform. The clipping of reads was performed using

385 Trimmomatic (v 0.36) and paired-end reads were merged using software FLASH2 (v 2.2.00) to obtain  
386 a single, longer read that covers the full target region. The processed reads were mapped, using  
387 BMWA MEM (v 0.7.15), to the reference sequence (the wild type *KRT14* exon1 sequence) with  
388 default alignment parameters. Only high quality, merged, on target reads were considered for further  
389 processing. Finally, the identification and quantification of sequences alleles using CRISPResso (v  
390 1.0.13) occurred. The NGS raw data are available in Gene Expression Omnibus with accession  
391 number GSE246345.

### 392 **Clonal analysis**

393 Sub-confluent keratinocytes mass cultures were trypsinized and 0,5-1 cell was plated into each well  
394 of a 96-well plate after serial dilution. After 7 days of cultivation, single clones were identified under  
395 an inverted microscope and treated with 0,05% trypsin and 0,01% EDTA at 37° for 15-20 minutes.  
396 One quarter of the clone was plated onto a 100mm indicator dish, cultivated for 12 days and stained  
397 with Rhodamine B for the classification of clonal type. The remaining three quarter was sub-  
398 cultivated on an adequate plastic support and used for further analyses.<sup>34</sup>

### 399 **Immunofluorescence**

400 Keratinocytes were plated at 2500 cell/well onto glass coverslips. After the formation of small  
401 colonies, cells were fixed with ice cold Methanol-Acetone (1:1) at -20°C for 10 minutes. Cells were  
402 permeabilized with PBS/Triton 0,5% for 15 minutes. Blocking solution (BSA 5%, 0.3% Triton in 1X  
403 PBS) was added for 30 minutes at 37°C and sections were incubated with primary and secondary  
404 antibody (Table S1). Cell nuclei were stained with DAPI. Fluorescence signals were monitored under  
405 a Zeiss AXIO Imager A.1 Manual Operation Fluorescence Microscope with EC Plan-Neofluar  
406 40X/0,75 objective.

### 407 **GUIDE-seq analysis**

408 5 x 10<sup>5</sup> primary EBS01 keratinocytes were nucleofected (as described in RNP paragraph) with the  
409 RNP complex and 40nM of the annealed dsODN. Treated keratinocytes were then plated (4-6 x 10<sup>3</sup>  
410 cells/cm<sup>2</sup>) on lethally irradiated 3T3-J2 cells and cultured until sub-confluence. Keratinocytes'  
411 genomic DNA was extracted and 14µg was sent to Creative Biogene for GUIDE-seq library  
412 preparation, sequencing in order to identify RGN (CRISPR RNA-guided nucleases)-dependent and -  
413 independent genomic breakpoint "hotspots". DNA library was sequenced using Illumina Miseq. The  
414 subsequent datasets were analysed using the *GUIDEseq* Bioconductor package software.

415 **Encapsulation with 10X Genomics chromium system and bioinformatic analysis on single-cell**  
416 **RNA-seq data**

417 Fully confluent keratinocytes were detached and cells were accurately resuspended to obtain a single  
418 cell suspension. About 10.000 cells of each eEBS01 and EBS01 samples were loaded into two  
419 channels of the Chromium Chip B using the Single Cell reagent kit v3.1 (10X Genomic) for Gel bead  
420 Emulsion generation. Following capture and lysis, cDNA was synthesized and amplified. Fifty  
421 nanograms of the amplified cDNA were then used for each sample to construct Illumina sequencing  
422 libraries. Sequencing was performed on the NextSeq550 Illumina sequencing platform following the  
423 10X Genomics instruction for read generation, reaching at least 50000 reads as mean reads per cell.

424 For the bioinformatic analysis, the Cell Ranger pipeline (version 3.1.0) was used to generate FASTQ  
425 files, to align reads to the reference transcriptome (GRCh38) and to calculate UMI counts from the  
426 mapped reads. Expression data were imported in R version 3.6.3 and analyzed using Seurat<sup>54</sup> (version  
427 3.1.5) R package. Cells were classified using an annotated scRNA-seq dataset of human  
428 keratinocytes<sup>28</sup> as reference and the FindTransferAnchors and TransferData functions in Seurat with  
429 default parameters. We assessed the quality of the assigned labels monitoring the expression of known  
430 markers. Expression data are available in Gene Expression Omnibus with accession number  
431 GSE246345.

**432 Heat shock assay**

433 Keratinocytes were plated at 10000 cell/well onto glass coverslip. Cells culture medium was replaced  
434 with KGM medium at 43°C and the well plate was immediately placed in a water bath set at 47°C.  
435 After 15 minutes of heat stress, the medium was immediately replaced with fresh KGM medium at  
436 37°C and the cells were allowed to recover in the incubator at 37°C, 5% CO<sub>2</sub> in humidified  
437 atmosphere. Coverslips were removed at 15-minute intervals thereafter and immunostained.

**438 Dispase-based keratinocyte dissociation assay (DDA)**

439  $4-6 \times 10^3$  cells/cm<sup>2</sup> keratinocytes were plated, on lethally irradiated 3T3-J2 cells onto a 6 well plate  
440 and cultured. After 20 days, the epidermal sheets were washed with grafting wash and incubated with  
441 Dispase II (Roche, #0494207801), 2,5U/ml diluted in PBS, for 1 hour at 37°C. After detachment, one  
442 sheet was subjected to low force stress with orbital rotation (200 rpm) for 5 minutes at 37°C and the  
443 other monolayer was transferred in a 15ml Falcon tube with 5ml of 1X PBS and exposed to high  
444 mechanical stress by 20-50 inversions. Fragments count was performed with ImageJ.

**445 Decellularized dermal matrixes preparation, cryopreservation and sectioning.**

446 Decellularized human dermal matrixes were obtained using human skin samples from surgical waste  
447 (abdominoplasty or mammoplasty). Briefly, skin biopsies were sectioned in fragments of  
448 approximately 1,5 cm<sup>2</sup>, immersed in sterile PBS at 60°C for thirty seconds under constant stirring  
449 and then in sterile cold PBS for 1 minute. The epidermis was then mechanically detached from the  
450 dermis using forceps. After decellularization, samples were rinsed in KGM for 24 hours. The  
451 following day, the decellularized dermal matrixes were seeded with primary human keratinocytes ( $1$   
452  $\times 10^5$  cells per scaffold) onto lethally irradiated 3T3-J2 cells ( $5 \times 10^4$  cells per scaffold) in KGM.  
453 After 10 days in submerged culture, the media was carefully removed, and the samples were gently  
454 moved in millicell® cell culture (Merk) and were further cultured for 20-24 days in air-liquid interface  
455 (ALI) condition to induce epidermal differentiation. 3D human skin equivalents were dehydrated in

456 a sucrose gradient 0.9M and 2M for thirty minutes respectively at RT, embedded in Killik-OCT  
457 cryostat embedding medium (Bio-Optica) and frozen. 7µm sections of embedded skin equivalents  
458 were obtained with a histological cryomicrotome (Leica CM1850 UV).

#### 459 **Haematoxylin and eosin staining.**

460 Hematoxylin and eosin staining was performed on 7µm cryosections of decellularized dermal  
461 matrixes (Harris haematoxylin for 1 min, running tap water for 1 min, eosin Y 50% in ethanol for  
462 thirty seconds, 95% ethanol for 1 min, 100% ethanol for 1 min, two rinses in fresh 100% ethanol for  
463 1 min each) and observed with Zeiss Microscope Axio Imager M2 with an EC Plan-Neofluar 10X/0.3  
464 M27 air objective.

465

#### 466 **Acknowledgments**

467 This project was supported by the European Research Council (ERC) Advanced Grant HOLO-GT  
468 (No. 101019289) and Telethon (Grant number: GGP20088). We thank Le ali di Camilla for providing  
469 assistance to patients.

470

#### 471 **Author Contributions**

472 C.C. performed experiments, analyzed data, assembled all input data. E.E. defined single cells RNA  
473 seq analyses and revised the manuscript. L.D.R. defined and analyzed functional assay and revised  
474 the manuscript. L.S. performed 3D skin equivalent assays. F.C. performed clonal analysis. M.F. and  
475 S.B. conducted bioinformatics analyses. A.P. performed protein structure prediction and modeling.  
476 G.B. made scRNA-seq library. E.T. performed NGS to identify gene variants. A. Paganelli, C.F. and  
477 C.M. provided EBS01 patient clinical management. M.C.L. and M.D.L. coordinated the study,  
478 defined strategic procedures, administered the experiments, and wrote the manuscript.

479

480 **Conflict of Interest**

481 M.D.L. is co-founder and member of the Board of Directors of Holostem Terapie Avanzate (HTA)  
482 s.r.l in liquidation, Modena, Italy, as well as consultants for J-TEC-Japan Tissue Engineering, Ltd.

483 The other authors state no conflict of interest.

484

485 **Keywords**

486 Epidermolysis bullosa, genetic disease, gene therapy, stem cells, keratinocytes biology, gene editing

487

488 **Data Availability Statement**

489 Data availability Sequencing data have been deposited to Gene Expression Omnibus with accession  
490 number GSE246345. We declare that the data supporting the findings of this study are available  
491 within the paper and its Supplementary Information Files or from the authors upon request.

492

493 **References**

- 494 1. Coulombe, P.A., Kerns, M.L., and Fuchs, E. (2009). Epidermolysis bullosa simplex: a paradigm  
495 for disorders of tissue fragility. *J. Clin. Invest.* *119*, 1784–1793.
- 496 2. Chamcheu, J.C., Siddiqui, I.A., Syed, D.N., Adhami, V.M., Liovic, M., and Mukhtar, H. (2011).  
497 Keratin gene mutations in disorders of human skin and its appendages. *Arch. Biochem. Biophys.*  
498 *508*, 123–137.
- 499 3. Fine, J.-D., Bruckner-Tuderman, L., Eady, R.A.J., Bauer, E.A., Bauer, J.W., Has, C., Heagerty,  
500 A., Hintner, H., Hovnanian, A., Jonkman, M.F., et al. (2014). Inherited epidermolysis bullosa:

- 501 Updated recommendations on diagnosis and classification. *J. Am. Acad. Dermatol.* 70, 1103–  
502 1126.
- 503 4. Fine, J.-D., Eady, R.A.J., Bauer, E.A., Bauer, J.W., Bruckner-Tuderman, L., Heagerty, A.,  
504 Hintner, H., Hovnanian, A., Jonkman, M.F., Leigh, I., et al. (2008). The classification of inherited  
505 epidermolysis bullosa (EB): Report of the Third International Consensus Meeting on Diagnosis  
506 and Classification of EB. *J. Am. Acad. Dermatol.* 58, 931–950.
- 507 5. Sprecher, E. (2010). Epidermolysis Bullosa Simplex. *Dermatol. Clin.* 28, 23–32.
- 508 6. Bauer, J.W., Koller, J., Murauer, E.M., De Rosa, L., Enzo, E., Carulli, S., Bondanza, S., Recchia,  
509 A., Muss, W., Diem, A., et al. (2017). Closure of a Large Chronic Wound through Transplantation  
510 of Gene-Corrected Epidermal Stem Cells. *J. Invest. Dermatol.* 137, 778–781.
- 511 7. De Rosa, L., Enzo, E., Zardi, G., Bodemer, C., Magnoni, C., Schneider, H., and De Luca, M.  
512 (2021). Hologene 5: A Phase II/III Clinical Trial of Combined Cell and Gene Therapy of  
513 Junctional Epidermolysis Bullosa. *Front. Genet.* 12, 705019.
- 514 8. De Rosa, L., Carulli, S., Cocchiarella, F., Quaglino, D., Enzo, E., Franchini, E., Giannetti, A.,  
515 De Santis, G., Recchia, A., Pellegrini, G., et al. (2014). Long-Term Stability and Safety of  
516 Transgenic Cultured Epidermal Stem Cells in Gene Therapy of Junctional Epidermolysis Bullosa.  
517 *Stem Cell Rep.* 2, 1–8.
- 518 9. Eichstadt, S., Tang, J.Y., Solis, D.C., Siprashvili, Z., Marinkovich, M.P., Whitehead, N., Schu,  
519 M., Fang, F., Erickson, S.W., Ritchey, M.E., et al. (2019). From Clinical Phenotype to Genotypic  
520 Modelling: Incidence and Prevalence of Recessive Dystrophic Epidermolysis Bullosa (RDEB).  
521 *Clin. Cosmet. Investig. Dermatol. Volume 12*, 933–942.

- 522 10. Hirsch, T., Rothoefl, T., Teig, N., Bauer, J.W., Pellegrini, G., De Rosa, L., Scaglione, D.,  
523 Reichelt, J., Klausegger, A., Kneisz, D., et al. (2017). Regeneration of the entire human epidermis  
524 using transgenic stem cells. *Nature* 551, 327–332.
- 525 11. Kueckelhaus, M., Rothoefl, T., De Rosa, L., Yeni, B., Ohmann, T., Maier, C., Eitner, L., Metze,  
526 D., Losi, L., Secone Seconetti, A., et al. (2021). Transgenic Epidermal Cultures for Junctional  
527 Epidermolysis Bullosa — 5-Year Outcomes. *N. Engl. J. Med.* 385, 2264–2270.
- 528 12. Mavilio, F., Pellegrini, G., Ferrari, S., Di Nunzio, F., Di Iorio, E., Recchia, A., Maruggi, G.,  
529 Ferrari, G., Provasi, E., Bonini, C., et al. (2006). Correction of junctional epidermolysis bullosa  
530 by transplantation of genetically modified epidermal stem cells. *Nat. Med.* 12, 1397–1402.
- 531 13. Siprashvili, Z., Nguyen, N.T., Gorell, E.S., Loutit, K., Khuu, P., Furukawa, L.K., Lorenz, H.P.,  
532 Leung, T.H., Keene, D.R., Rieger, K.E., et al. (2016). Safety and Wound Outcomes Following  
533 Genetically Corrected Autologous Epidermal Grafts in Patients With Recessive Dystrophic  
534 Epidermolysis Bullosa. *JAMA* 316, 1808.
- 535 14. Chakravarti, S., Enzo, E., Rocha Monteiro de Barros, M., Maffezzoni, M.B.R., and Pellegrini, G.  
536 (2022). Genetic Disorders of the Extracellular Matrix: From Cell and Gene Therapy to Future  
537 Applications in Regenerative Medicine. *Annu. Rev. Genomics Hum. Genet.* 23, 193–222. 10.
- 538 15. Jumper, J., Evans, R., Pritzel, A., Green, T., Figurnov, M., Ronneberger, O., Tunyasuvunakool,  
539 K., Bates, R., Žídek, A., Potapenko, A., et al. (2021). Highly accurate protein structure prediction  
540 with AlphaFold. *Nature* 596, 583–589.
- 541 16. Lee, C.-H., Kim, M.-S., Chung, B.M., Leahy, D.J., and Coulombe, P.A. (2012). Structural basis  
542 for heteromeric assembly and perinuclear organization of keratin filaments. *Nat. Struct. Mol.*  
543 *Biol.* 19, 707–715.

- 544 17. Rugg, E.L., Morley, S.M., Smith, F.J.D., Boxer, M., Tidman, M.J., Navsaria, H., Leigh, I.M., and  
545 Lane, E.B. (1993). Missing links: Weber–Cockayne keratin mutations implicate the L12 linker  
546 domain in effective cytoskeleton function. *Nat. Genet.* 5, 294–300.
- 547 18. Parry, D.A.D., Marekov, L.N., Steinert, P.M., and Smith, T.A. (2002). A Role for the 1A and L1  
548 Rod Domain Segments in Head Domain Organization and Function of Intermediate Filaments:  
549 Structural Analysis of Trichocyte Keratin. *J. Struct. Biol.* 137, 97–108.
- 550 19. Charlesworth, C.T., Deshpande, P.S., Dever, D.P., Camarena, J., Lemgart, V.T., Cromer, M.K.,  
551 Vakulskas, C.A., Collingwood, M.A., Zhang, L., Bode, N.M., et al. (2019). Identification of  
552 preexisting adaptive immunity to Cas9 proteins in humans. *Nat. Med.* 25, 249–254.
- 553 20. Batta, K., Rugg, E.L., Wilson, N.J., West, N., Goodyear, H., Lane, E.B., Gratian, M., Dopping-  
554 Hepenstal, P., Moss, C., and Eady, R.A.J. (2000). A keratin 14 ‘knockout’ mutation in recessive  
555 epidermolysis bullosa simplex resulting in less severe disease. *Br. J. Dermatol.*, 7.
- 556 21. Yiasemides, E., Trisnowati, N., Su, J., Dang, N., Klingberg, S., Marr, P., Melbourne, W., Tran,  
557 K., Chow, C.W., Orchard, D., et al. (2008). Clinical heterogeneity in recessive epidermolysis  
558 bullosa due to mutations in the keratin 14 gene, *KRT14*. *Clin. Exp. Dermatol.* 33, 689–697.
- 559 22. Sørensen, C.B., Andresen, B.S., Jensen, U.B., Jensen, T.G., Jensen, P.K.A., Gregersen, N., and  
560 Bolund, L. (2003). Functional testing of keratin 14 mutant proteins associated with the three  
561 major subtypes of epidermolysis bullosa simplex. *Exp. Dermatol.* 12, 472–479.
- 562 23. Tan, T.S., Ng, Y.Z., Badowski, C., Dang, T., Common, J.E.A., Lacina, L., Szeverényi, I., and  
563 Lane, E.B. (2016). Assays to Study Consequences of Cytoplasmic Intermediate Filament  
564 Mutations. In *Methods in Enzymology* (Elsevier), pp. 219–253.

- 565 24. Morley, S.M., Dundas, S.R., James, J.L., Gupta, T., Brown, R.A., Sexton, C.J., Navsaria, H.A.,  
566 Leigh, I.M., and Lane, E.B. (1995). Temperature sensitivity of the keratin cytoskeleton and  
567 delayed spreading of keratinocyte lines derived from EBS patients. *J. Cell Sci.* *108*, 3463–3471.
- 568 25. Coulombe, P.A., Hutton, M.E., Letal, A., Hebert, A., Paller, A.S., and Fuchs, E. (1991). Point  
569 mutations in human keratin 14 genes of epidermolysis bullosa simplex patients: Genetic and  
570 functional analyses. *Cell* *66*, 1301–1311.
- 571 26. Kitajima, Y., Inoue, S., and Yaoita, H. (1989). Abnormal organization of keratin intermediate  
572 filaments in cultured keratinocytes of epidermolysis bullosa simplex. *Arch. Dermatol. Res.* *281*,  
573 5–10.
- 574 27. Barrandon, Y., and Green, H. (1987). Three clonal types of keratinocyte with different capacities  
575 for multiplication. *Proc. Natl. Acad. Sci.* *84*, 2302–2306.
- 576 28. Enzo, E., Secone Seconetti, A., Forcato, M., Tenedini, E., Polito, M.P., Sala, I., Carulli, S.,  
577 Contin, R., Peano, C., Tagliafico, E., et al. (2021). Single-keratinocyte transcriptomic analyses  
578 identify different clonal types and proliferative potential mediated by FOXM1 in human  
579 epidermal stem cells. *Nat. Commun.* *12*, 2505.
- 580 29. Pellegrini, G., Golisano, O., Paterna, P., Lambiase, A., Bonini, S., Rama, P., and De Luca, M.  
581 (1999). Location and Clonal Analysis of Stem Cells and Their Differentiated Progeny in the  
582 Human Ocular Surface. *J. Cell Biol.* *145*, 769–782.
- 583 30. Rochat, A., Kobayashi, K., and Barrandon, Y. (1994). Location of stem cells of human hair  
584 follicles by clonal analysis. *Cell* *76*, 1063–1073.
- 585 31. Polito, M.P., Marini, G., Palamenghi, M., and Enzo, E. (2023). Decoding the Human Epidermal  
586 Complexity at Single-Cell Resolution. *Int. J. Mol. Sci.* *24*, 8544.

- 587 32. De Rosa, L., Enzo, E., Palamenghi, M., Sercia, L., and Luca, M.D. (2023). Stairways to Advanced  
588 Therapies for Epidermolysis Bullosa. *Cold Spring Harb Perspect Biol* 15(4).
- 589 33. Rama, P., Matuska, S., Paganoni, G., Spinelli, A., De Luca, M., and Pellegrini, G. (2010). Limbal  
590 Stem-Cell Therapy and Long-Term Corneal Regeneration. *N. Engl. J. Med.* 363, 147–155.
- 591 34. Enzo, E., Cattaneo, C., Consiglio, F., Polito, M.P., Bondanza, S., and De Luca, M. (2022). Clonal  
592 analysis of human clonogenic keratinocytes. In *Methods in Cell Biology* (Elsevier), pp. 101–116.
- 593 35. Bolling, M.C., Lemmink, H.H., Jansen, G.H.L., and Jonkman, M.F. (2011). Mutations in KRT5  
594 and KRT14 cause epidermolysis bullosa simplex in 75% of the patients: KRT5 and KRT14  
595 mutations in 75% of EBS patients. *Br. J. Dermatol.*, 637–44.
- 596 36. György, B., Nist-Lund, C., Pan, B., Asai, Y., Karavitaki, K.D., Kleinstiver, B.P., Garcia, S.P.,  
597 Zaborowski, M.P., Solanes, P., Spataro, S., et al. (2019). Allele-specific gene editing prevents  
598 deafness in a model of dominant progressive hearing loss. *Nat. Med.* 25, 1123–1130.
- 599 37. Latella, M.C., Di Salvo, M.T., Cocchiarella, F., Benati, D., Grisendi, G., Comitato, A., Marigo,  
600 V., and Recchia, A. (2016). In vivo Editing of the Human Mutant Rhodopsin Gene by  
601 Electroporation of Plasmid-based CRISPR/Cas9 in the Mouse Retina. *Mol. Ther. - Nucleic Acids*  
602 5, e389.
- 603 38. Kocher, T., Peking, P., Klausegger, A., Muraue, E.M., Hofbauer, J.P., Wally, V., Lettner, T.,  
604 Hainzl, S., Ablinger, M., Bauer, J.W., et al. (2017). Cut and Paste: Efficient Homology-Directed  
605 Repair of a Dominant Negative KRT14 Mutation via CRISPR/Cas9 Nickases. *Mol. Ther.* 25,  
606 2585–2598.
- 607 39. March, O.P., Lettner, T., Klausegger, A., Ablinger, M., Kocher, T., Hainzl, S., Peking, P.,  
608 Lackner, N., Rajan, N., Hofbauer, J.P., et al. (2019). Gene Editing–Mediated Disruption of

- 609 Epidermolytic Ichthyosis–Associated KRT10 Alleles Restores Filament Stability in  
610 Keratinocytes. *J. Invest. Dermatol.* *139*, 1699-1710.
- 611 40. Luan, X.-R., Chen, X.-L., Tang, Y.-X., Zhang, J.-Y., Gao, X., Ke, H.-P., Lin, Z.-Y., and Zhang,  
612 X.-N. (2018). CRISPR/Cas9-Mediated Treatment Ameliorates the Phenotype of the  
613 Epidermolytic Palmoplantar Keratoderma-like Mouse. *Mol. Ther. - Nucleic Acids* *12*, 220–228.
- 614 41. Aushev, M., Koller, U., Mussolino, C., Cathomen, T., and Reichelt, J. (2017). Traceless Targeting  
615 and Isolation of Gene-Edited Immortalized Keratinocytes from Epidermolysis Bullosa Simplex  
616 Patients. *Mol. Ther. - Methods Clin. Dev.* *6*, 112–123.
- 617 42. Webber, B.R., Osborn, M.J., McElroy, A.N., Twaroski, K., Lonetree, C., DeFeo, A.P., Xia, L.,  
618 Eide, C., Lees, C.J., McElmurry, R.T., et al. (2016). CRISPR/Cas9-based genetic correction for  
619 recessive dystrophic epidermolysis bullosa. *Npj Regen. Med.* *1*, 16014.
- 620 43. Hainzl, S., Peking, P., Kocher, T., Muraier, E.M., Larcher, F., Del Rio, M., Duarte, B., Steiner,  
621 M., Klausegger, A., Bauer, J.W., et al. (2017). COL7A1 Editing via CRISPR/Cas9 in Recessive  
622 Dystrophic Epidermolysis Bullosa. *Mol. Ther.* *25*, 2573–2584.
- 623 44. Wu, W., Lu, Z., Li, F., Wang, W., Qian, N., Duan, J., Zhang, Y., Wang, F., and Chen, T. (2017).  
624 Efficient in vivo gene editing using ribonucleoproteins in skin stem cells of recessive dystrophic  
625 epidermolysis bullosa mouse model. *Proc. Natl. Acad. Sci.* *114*, 1660–1665.
- 626 45. Danner, E., Bashir, S., Yumlu, S., Wurst, W., Wefers, B., and Kühn, R. (2017). Control of gene  
627 editing by manipulation of DNA repair mechanisms. *Mamm. Genome* *28*, 262–274.
- 628 46. Nelson, J.W., Randolph, P.B., Shen, S.P., Everette, K.A., Chen, P.J., Anzalone, A.V., An, M.,  
629 Newby, G.A., Chen, J.C., Hsu, A., et al. (2022). Engineered pegRNAs improve prime editing  
630 efficiency. *Nat. Biotechnol.* *40*, 402–410.

- 631 47. Petri, K., Zhang, W., Ma, J., Schmidts, A., Lee, H., Horng, J.E., Kim, D.Y., Kurt, I.C., Clement,  
632 K., Hsu, J.Y., et al. (2022). CRISPR prime editing with ribonucleoprotein complexes in zebrafish  
633 and primary human cells. *Nat. Biotechnol.* *40*, 189–193.
- 634 48. Huang, T.P., Newby, G.A., and Liu, D.R. (2021). Precision genome editing using cytosine and  
635 adenine base editors in mammalian cells. *Nat. Protoc.* *16*, 1089–1128.
- 636 49. Antoniou, P., Hardouin, G., Martinucci, P., Frati, G., Felix, T., Chalumeau, A., Fontana, L.,  
637 Martin, J., Masson, C., Brusson, M., et al. (2022). Base-editing-mediated dissection of a  $\gamma$ -globin  
638 cis-regulatory element for the therapeutic reactivation of fetal hemoglobin expression. *Nat.*  
639 *Commun.* *13*, 6618.
- 640 50. Kleinstiver, B.P., Sousa, A.A., Walton, R.T., Tak, Y.E., Hsu, J.Y., Clement, K., Welch, M.M.,  
641 Horng, J.E., Malagon-Lopez, J., Scarfò, I., et al. (2019). Engineered CRISPR–Cas12a variants  
642 with increased activities and improved targeting ranges for gene, epigenetic and base editing. *Nat.*  
643 *Biotechnol.* *37*, 276–282.
- 644 51. Strecker, J., Jones, S., Koopal, B., Schmid-Burgk, J., Zetsche, B., Gao, L., Makarova, K.S.,  
645 Koonin, E.V., and Zhang, F. (2019). Engineering of CRISPR-Cas12b for human genome editing.  
646 *Nat. Commun.* *10*, 212.
- 647 52. McMahon, M.A., Prakash, T.P., Cleveland, D.W., Bennett, C.F., and Rahdar, M. (2018).  
648 Chemically Modified Cpf1-CRISPR RNAs Mediate Efficient Genome Editing in Mammalian  
649 Cells. *Mol. Ther.* *26*, 1228–1240.
- 650 53. Todaro, G.J., Green, H., and Goldberg, B.D. (1964). TRANSFORMATION OF PROPERTIES  
651 OF AN ESTABLISHED CELL LINE BY SV40 AND POLYOMA VIRUS. *Proc. Natl. Acad.*  
652 *Sci.* *51*, 66–73.

653 54. Stuart, T., Butler, A., Hoffman, P., Hafemeister, C., Papalexi, E., Mauck, W.M., Hao, Y.,  
654 Stoeckius, M., Smibert, P., and Satija, R. (2019). Comprehensive Integration of Single-Cell Data.  
655 *Cell* 177, 1888-1902.

656

## 657 **Figures legends**

### 658 **Figure 1: A novel monoallelic *KRT14* deletion causing a dominant form of Epidermolysis** 659 **bullosa simplex**

660 **A)** Clinical images of the patient EBS01: bullous lesions are present on the palmoplantar region.  
661 Unremitting blister on the heel, dorsal medial part of the left foot and right peri-malleolar region are  
662 shown in the panel below. **B)** Amino acid sequence of the wild-type and mutant K14. The invariant  
663 residues are displayed in black boxes and the red box highlights the mutant region with the 7 amino  
664 acids deletion. The secondary structures are represented above the sequences as ribbons (helices)  
665 and arrows (strands), respectively; blanks indicate unassigned regions. The Head and Tail domains  
666 of *KRT14* are represented as N-terminal and C-terminal grey boxes, respectively. Coil and Linker  
667 regions are represented as yellow and cyan boxes, respectively. **C)** Predicted three-dimensional  
668 structures of human wild-type (yellow) and mutant (grey) K14 protein. The lack of the Linker 1  
669 region, which is visible in the c475/495del21 protein, is circled in red.

### 670 **Figure 2: Gene-editing of *KRT14* mutated allele**

671 **A)** Representation of the EBS01 patient's genotype and allele profile of *KRT14* gene on human  
672 chromosome 17. The expanded section of the exon 1 illustrates the 21 nucleotides absent in *KRT14*  
673 exon 1 mutant allele (light blue). Mutant allele specific guide RNA is depicted in purple, straddling  
674 both the terminal sides of the deletion, and the -AGG- PAM sequence in red. **B)** Graphic  
675 representation of TIDE analysis. Both the wild-type and mutant allele were detected in the untreated  
676 sample (EBS01). In the treated sample (eEBS01) the mutant allele has been deleted by gene editing.

677 **D)** Histogram representation of NGS analysis of three technical replicates post gene editing. Edited  
678 and not edited percentages on both wild-type and mutant alleles are calculated on the total number  
679 of reads. **D)** PCR analysis of three technical replicates (EXP1, EXP2, EXP3). For each experiment,  
680 a PCR product was amplified both from the EBS01 and eEBS01 keratinocytes' genome with primers  
681 specific to anneal to wild-type (268 bp) and mutant alleles (266bp). **E)** Graphic representation of  
682 editing derived InDels in mutant *KRT14* allele (N= 3). **F)** NGS analysis of PCR products  
683 surrounding the Cas9 target sites in the genome of eEBS01 showed a wide variety of Indel mutations  
684 mediated by NHEJ at the targeted exon 1. The top sequence is the mutant allele unmodified  
685 sequence, the dotted line represents the Cas9 cleavage upstream of the PAM.

### 686 **Figure 3: Restoration of intermediate filaments**

687 **A)** Immunofluorescent staining of K14 intermediate filaments in healthy donor derived  
688 keratinocytes (NHEK), untreated and treated EBS01 keratinocytes (EBS01 and eEBS01  
689 respectively). Nuclei are stained in blue by DAPI. Scale bar= 20 $\mu$ m. **B)** Immunofluorescent staining  
690 of K14 filament before and after heat shock assay. At time 0 and after 15 minutes recovery from  
691 heat shock, NHEK and eEBS01 do not show any changes in the organization of cytoplasmatic  
692 network, whereas EBS01 keratinocytes display disruption of intermediate filament also in the  
693 perinuclear region. After 60 minutes recovery, EBS01 intermediate filament aggregates revert to a  
694 condition similar to that before the heat shock. Nuclei are stained in blue by DAPI. Scale bar=  
695 20 $\mu$ m. **C)** Dispase-mediated epidermal sheet dissociation assay of NHEK, EBS01 and eEBS01  
696 epidermal cultures before (C) and after (D) mechanical stress. No fragmentation was detected in  
697 samples subjected to low-force orbital rotation. In contrast, high force stress induced fragmentation  
698 of EBS01, but not NHEK and eEBS01 sheets (**D**). **E)** Number of fragments derived from each  
699 sample has been counted using ImageJ software and unpaired t-test showed a statistically significant  
700 P-value between EBS01 and eEBS01 number of fragments (N=3; asterisk indicate P-value<0,05).

### 701 **Figure 4: 3D skin equivalents**

702 (A) Haematoxylin and eosin staining of sections (7- $\mu$ m thick) of decellularized dermal matrixes  
703 (Dermis) seeded with normal human epidermal keratinocytes (NHEK). (B) The decellularized  
704 dermal matrix was seeded with EBS01 or eEBS01 cells. Black arrowheads show blisters originated  
705 in the epidermal basal layer only in EBS01 3D cultures. Scale bar, 100 $\mu$ m.

706 **Figure 5: Genetic correction of epidermal stem cells**

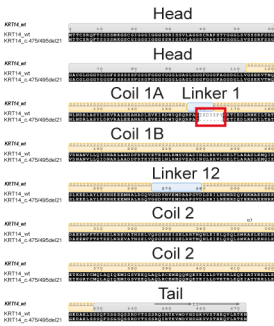
707 **A-B)** Uniform manifold approximation and projection (UMAP) of the scRNA-seq experiment.  
708 EBS01 and eEBS01 keratinocytes mass cultures were profiled, integrated and classified in all their  
709 clonogenic and differentiated clusters (H in red, M light blue, P grey, TD1 light brown, TD2 brown)  
710 Distribution and extension of the clusters are comparable between the two samples. Feeder layer  
711 derived fibroblast and low-quality keratinocytes are shown in light gray. **C)** Table shows the  
712 percentages of cells in each EBS01 and eEBS01 clusters after scRNA-seq analysis. This quantitative  
713 analysis demonstrates a comparable percentage between the treated and not treated samples. **D)**  
714 Graphical representation of clonal analysis assay results. Clonal population percentages represent the  
715 average value of Holoclones (H), Meroclones (M) and Paraclones (P) of two independent experiments  
716 (EBS01: Holoclones 5%, Meroclones 52%, Paraclones 43%; eEBS01: Holoclones 5%, Meroclones  
717 48%, Paraclones 47%). As shown, there are no differences in clonal populations between EBS01 and  
718 eEBS01 keratinocytes. **E)** Representative indicator dishes for EBS01 and eEBS01 Holoclones,  
719 Meroclones and Paraclones. **F)** PCR products of holoclones eEBS01's wild-type and mutant alleles.  
720 Wild-type alleles result untouched, whereas all the mutated alleles display editing and lack of primer  
721 annealing and amplification. Not treated EBS01 sample was used as control (CP) in which both the  
722 wild-type and mutant allele are present and amplified.

A



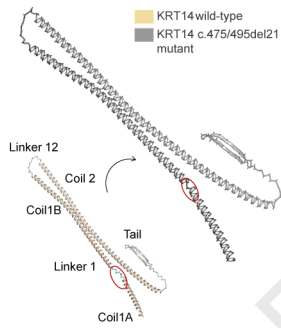
B

Keratin 14 amino acid sequence

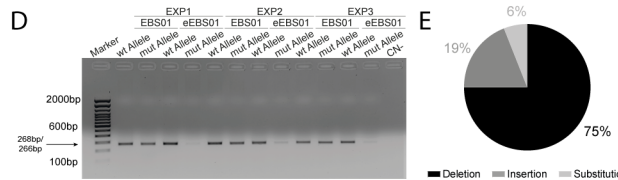
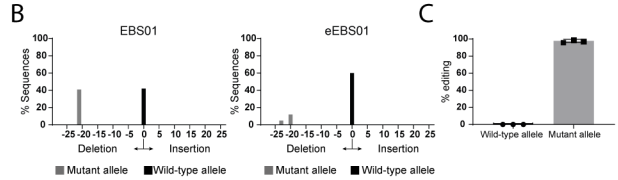
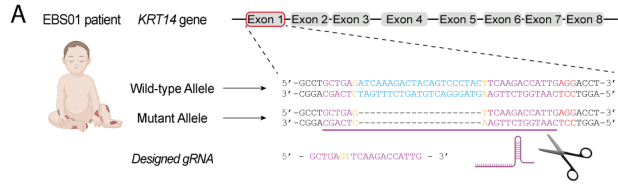


C

Keratin 14 protein structure

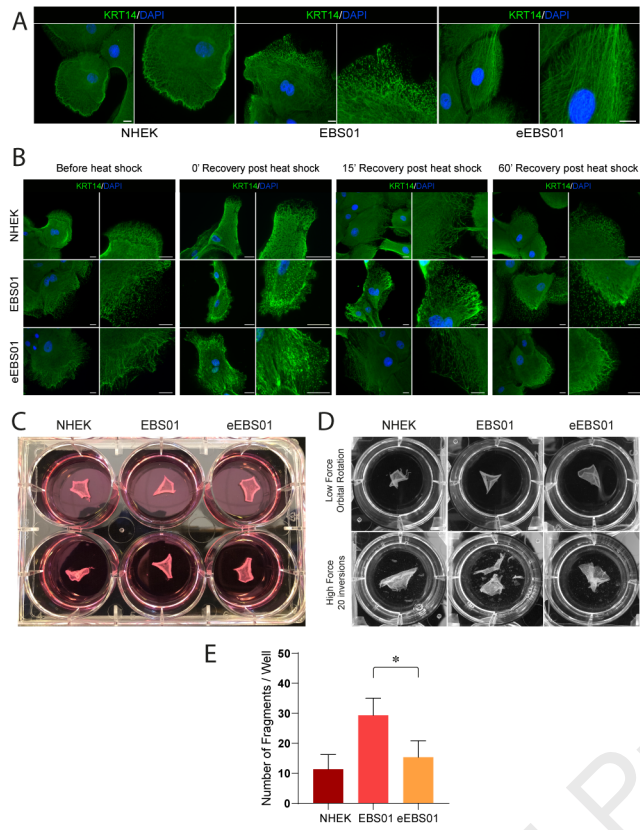


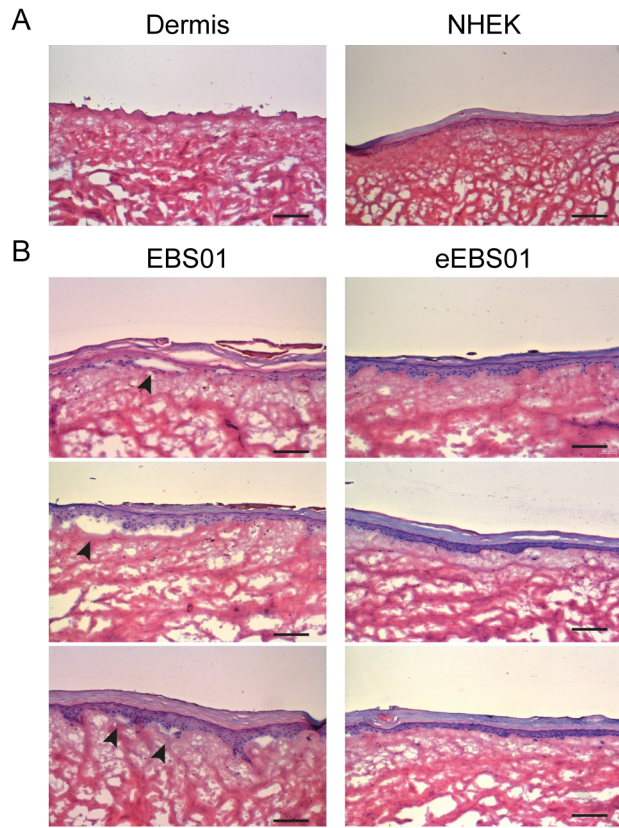
Journal Pre-proof

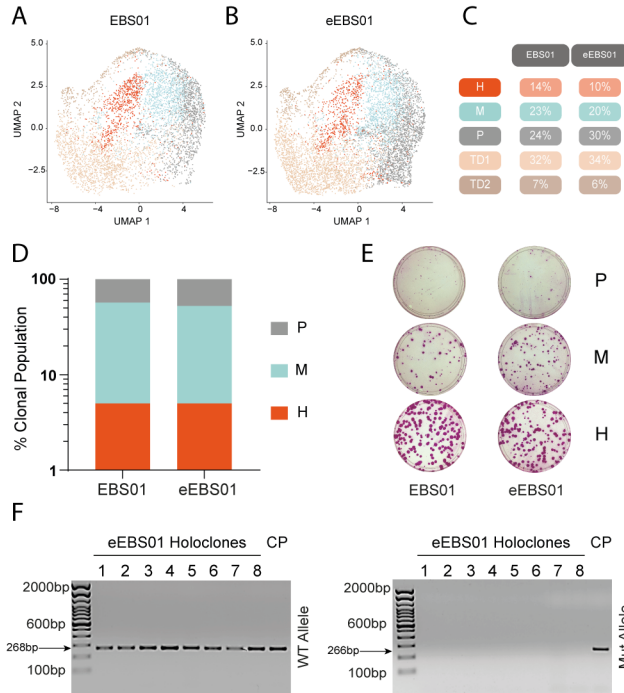


**F**

Reference mutant allele	Sequence
0.00%	G C C T G C T G A G T T C A A G A C C A T T G A G G A C C T G A G G A A C A A G
7.03%	G C C T G C T G A G T T C A A G A C C A T T G A G G A C C T G A G G A A C A A G
5.85%	G C C T G C T G A G T T C A A G A C C A T T G A G G A C C T G A G G A A C A A G
2.93%	G C C T G C T G A G T T C A A G A C C A T T G A G G A C C T G A G G A A C A A G
17.1%	G C C T G C T G A G T T C A A G A C C A T T G A G G A C C T G A G G A A C A A G
1.53%	G C C T G C T G A G T T C A A G A C C A T T G A G G A C C T G A G G A A C A A G
1.53%	G C C T G C T G A G T T C A A G A C C A T T G A G G A C C T G A G G A A C A A G
0.87%	G C C T G C T G A G T T C A A G A C C A T T G A G G A C C T G A G G A A C A A G
0.87%	G C C T G C T G A G T T C A A G A C C A T T G A G G A C C T G A G G A A C A A G
0.51%	G C C T G C T G A G T T C A A G A C C A T T G A G G A C C T G A G G A A C A A G
0.76%	G C C T G C T G A G T T C A A G A C C A T T G A G G A C C T G A G G A A C A A G
0.76%	G C C T G C T G A G T T C A A G A C C A T T G A G G A C C T G A G G A A C A A G
0.88%	G C C T G C T G A G T T C A A G A C C A T T G A G G A C C T G A G G A A C A A G
0.88%	G C C T G C T G A G T T C A A G A C C A T T G A G G A C C T G A G G A A C A A G
0.57%	G C C T G C T G A G T T C A A G A C C A T T G A G G A C C T G A G G A A C A A G
0.51%	G C C T G C T G A G T T C A A G A C C A T T G A G G A C C T G A G G A A C A A G
0.48%	G C C T G C T G A G T T C A A G A C C A T T G A G G A C C T G A G G A A C A A G
0.48%	G C C T G C T G A G T T C A A G A C C A T T G A G G A C C T G A G G A A C A A G
0.41%	G C C T G C T G A G T T C A A G A C C A T T G A G G A C C T G A G G A A C A A G
0.34%	G C C T G C T G A G T T C A A G A C C A T T G A G G A C C T G A G G A A C A A G
0.33%	G C C T G C T G A G T T C A A G A C C A T T G A G G A C C T G A G G A A C A A G
0.30%	G C C T G C T G A G T T C A A G A C C A T T G A G G A C C T G A G G A A C A A G







De Luca and colleagues propose an allele specific gene editing strategy for EBS01 patient affected by a rare skin disease inherited in an autosomal manner (EBS). This work aims to restore a normal cellular phenotype and a correct intermediate filament network in epidermal stem cells.

Journal Pre-proof